

## A Binuclear Fe(III)Dy(III) Single Molecule Magnet. Quantum Effects and Models

Marilena Ferbinteanu,<sup>\*,†,¶</sup> Takashi Kajiwara,<sup>†,§</sup> Kwang-Yong Choi,<sup>‡</sup> Hiroyuki Nojiri,<sup>‡</sup> Akio Nakamoto,<sup>#</sup> Norimichi Kojima,<sup>#</sup> Fanica Cimpoesu,<sup>\*,†,‡</sup> Yuichi Fujimura,<sup>†</sup> Shinya Takaishi,<sup>†</sup> and Masahiro Yamashita<sup>†,§</sup>

Department of Chemistry, Graduate School of Science, Tohoku University, Aramaki, Aoba-ku, Sendai 980-8578, Japan, Institute for Materials Research, Tohoku University, Katahira 2-1-1, Sendai 980-8577, Japan, Department of Basic Science, Graduate School of Arts and Sciences, The University of Tokyo, Komaba, Meguro-ku, Tokyo 113-8654, Japan, and CREST, Japan Science and Technology Agency (JST), Japan

Received April 7, 2006; E-mail: marilena@agnus.chem.tohoku.ac.jp

The growing number of reports under the Single Molecule Magnet (SMM)<sup>1</sup> paradigm and the variety of SMM systems demonstrates a rather large generality of the effect, demanding the rationalization of the driving factors. Due to the intrinsic magnetic anisotropy of given lanthanide ions, the investigation of *d*-*f* complexes is a rational way to SMMs. It offers challenging case studies (several large clusters,<sup>2</sup> a binuclear<sup>3</sup> and even *f* mono-nuclear, where a key role is played by the nuclear spins<sup>4</sup>).

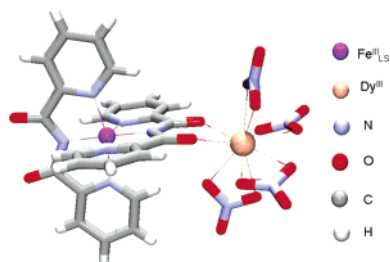


Figure 1. Molecular structure of [Fe(bpca)( $\mu$ -bpca)Dy(NO<sub>3</sub>)<sub>4</sub>] (1).

Here we bring a *d*-*f* binuclear SMM and a consistent insight with experimental and theoretical data. The isostructural series of [Fe<sup>III</sup><sub>LS</sub>(bpca)( $\mu$ -bpca)Ln<sup>III</sup>(NO<sub>3</sub>)<sub>4</sub>] binuclears was obtained from the

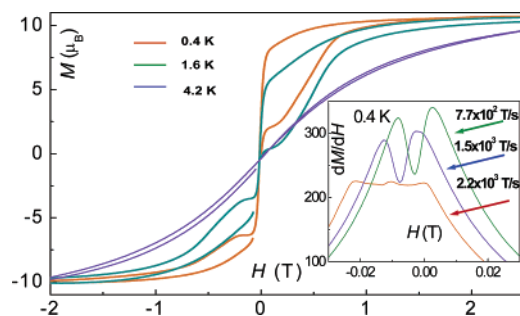


Figure 2. The field and temperature dependence of magnetization  $M$  for **1**. Inset: sweeping rate dependence of  $dM/dH$  near  $H = 0$  T at 0.4 K.

[Fe(bpca)<sub>2</sub>]<sup>+</sup> building block<sup>5</sup> (Hbpca = bis(2-pyridyl)carbonylamine) and Ln(NO<sub>3</sub>)<sub>3</sub> $\cdot$ *n*H<sub>2</sub>O (Ln = Eu, Gd, Tb, Dy, Ho). Related chain structures [Fe<sup>II</sup>( $\mu$ -bpca)<sub>2</sub>Ln(NO<sub>3</sub>)<sub>3</sub>(H<sub>2</sub>O)] with diamagnetic Fe<sup>II</sup>, without SMM effects, acting as a blank probe for lanthanide

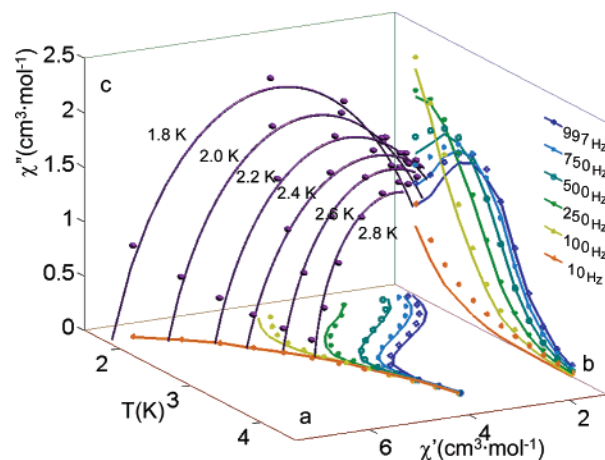


Figure 3. AC susceptibility measurement (marked points) and fit (lines) to a generalized Debye model (with  $\alpha = 0.05$ – $0.14$ ). Synoptic 3D view of: (a)  $\chi'$  versus  $T$ , (b)  $\chi''$  versus  $T$ , and (c)  $\chi'$  versus  $\chi''$  (Cole–Cole diagrams at various  $T$ ).

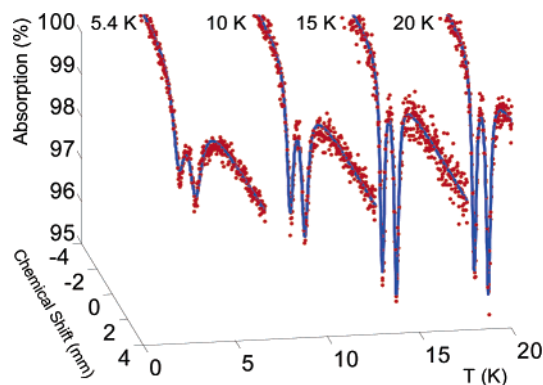


Figure 4. The low spin (LS) Fe(III) Mössbauer resonances and the anomalous temperature dependence due to the onset of magnetic ordering.

magnetism in comparison to the Fe<sup>III</sup>Ln<sup>III</sup> systems were synthesized and characterized also. Herein we confine our study to the binuclear<sup>6</sup> [Fe<sup>III</sup>(bpca)( $\mu$ -bpca)Dy(NO<sub>3</sub>)<sub>4</sub>] (**1**), the other systems and a more detailed analysis being the subject of a further work. The mono-negative bpca<sup>-</sup> ligand acts as tridentate N donor toward the *d* ion, being also able to accomplish bridging function as bidentate O donor toward the *f* site (see Figure 1).

Low temperature magnetization measurements at fast sweeping pulsed field revealed hysteresis loops and step-like magnetization, indicating quantum tunneling effects (Figure 2). The  $dM/dH$  curve at 0.4 K and  $7.7 \times 10^2$  T/s sweeping rate shows peaks at 0.54,

<sup>†</sup> Graduate School of Science, Tohoku University.

<sup>‡</sup> Institute for Materials Research, Tohoku University.

<sup>#</sup> The University of Tokyo.

<sup>§</sup> CREST, JST.

<sup>¶</sup> Permanent address: University of Bucharest, Faculty of Chemistry, Department of Inorganic Chemistry, Dumbrava Rosie 23, Bucharest 70254, Romania.

<sup>‡</sup> Permanent address: Institute of Physical Chemistry, Splaiul Independentei 202, Bucharest 77208, Romania.

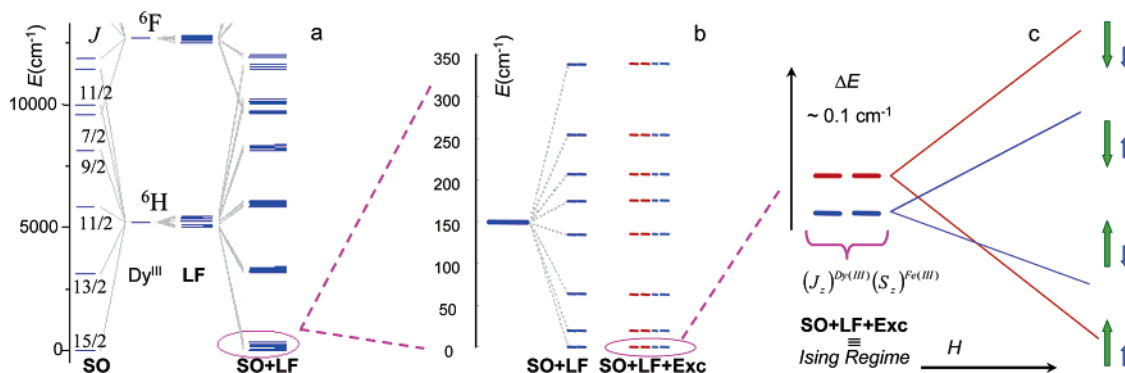


**Figure 5.** (a) The CASSCF calculation of the  ${}^6\text{H}$  and  ${}^6\text{F}$  terms of  $\text{Dy}^{\text{III}}$  free ion (left) and the LF versus LF + SO effects in  $[\text{Co}^{\text{III}}(\text{bpca})_2\text{Dy}(\text{NO}_3)_4]$  (right). (b) The split of  $J = 15/2$  set of  $\text{Dy}^{\text{III}}$  in  $\text{Co}^{\text{III}}(\text{bpca})_2\text{Dy}(\text{NO}_3)_4$  (LF + SO effects) and  $[\text{Fe}^{\text{III}}(\text{bpca})_2\text{Dy}(\text{NO}_3)_4]$  (LF + SO + Exc). The eight quasi-four-degenerate levels are in fact 16 two-degenerate ones with small exchange spacing. (c) Qualitative sketch of the field tuned crossing of the Ising-type levels of the  $\text{Fe}^{\text{III}}\text{Dy}^{\text{III}}$  complex.

0.29, 0.0028, and  $-0.0082$  T. The temperature and sweeping rate dependence of  $M$  versus  $H$  curves probe the nonadiabatic change of magnetization. The AC susceptibility measurements were carried out in a 3 G AC field oscillating at 10–1000 Hz, under a 0.1 T static field. The static field is tuning the system outside the fast tunneling regime. The in-phase ( $\chi'$ ) and out-of-phase ( $\chi''$ ) magnetic susceptibilities show the pattern of the slow relaxation of magnetization, probing the SMM nature of **1**. The  $\chi'$  versus  $\chi''$  at different  $T$  sections follows Cole–Cole semicircular profiles (Figure 3). The Arrhenius fit, with  $\ln(2\pi\nu) = -\ln(\tau_0) - \Delta/k_{\text{B}}T$ , of the  $(\nu, T)$  points representing the maxima of the  $\chi''$  versus  $T$  curves yielded the relaxation barrier  $\Delta = 8.98$   $\text{cm}^{-1}$  and time  $\tau_0 = 7.77 \times 10^{-8}$  s.

The unusual broadening of the Mössbauer signal at low temperatures is in line with the SMM behavior (Figure 4). The trend is due to the Zeeman splitting on the  $I = 1/2$  and  $3/2$  nuclear levels with the progressive onset of magnetic order (incomplete yet down to 4 K). The Mössbauer time scale,  $\sim 10^{-7}$  s, corroborates well with the above estimated  $\tau_0$ .

Ab initio calculations, CASSCF(14,10), were performed<sup>7</sup> in the  $(t_{2g})^5 + f^9$  active space of the  $d-f$  couple. The ab initio approach to the  $d-f$  systems is not straightforward,<sup>8</sup> due to their non-*aufbau* nature. The  $\text{Fe}(d^{5.77})\text{Dy}(d^{0.52}f^{9.00})$  populations, retrieving the  $f^9$  shell, tested the computational reliability. The spin-orbit (SO), ligand field (LF), and exchange (Exc) effects were implicitly accounted for. The computed SO matches well with the free ion spectrum, and the LF and LF + SO effects are also in accordance with the known experimental ranges.<sup>9</sup> The CASSCF + SO calculation for a  $\text{Co}^{\text{III}}\text{Dy}^{\text{III}}$  complex (Figure 5a,b) gave eight doubly degenerate pairs, in principle related to the  $\pm J_z$  components of the  $J = 15/2$  state on  $\text{Dy}^{\text{III}}$ . Driven by LF + SO factors, the pattern seems to be qualitatively similar to a zero field splitting, but is more complex quantitatively. The ab initio assignment of the  $J_z$  labels was not presently done.

The  $\text{Fe}^{\text{III}}\text{Dy}^{\text{III}}$  system (Figure 5b) shows eight sets of quasi-four-degenerate levels, whose small splitting ( $0.015$   $\text{cm}^{-1}$  on average) can be assimilated to the Ising pattern,  $J_{\text{df}}S_zJ_z$ . The ab initio analysis reliably reveals the mechanism and the range of coupling, but the absolute magnitude of the Ising gaps is below the practicable precision. Then, using experimental information and assigning the 0.54 T tunneling step (Figure 2) to the ground-state curve crossing (Figure 5c), one estimates  $J_{\text{df}} = -0.07$   $\text{cm}^{-1}$ . The magnetization plateau (Figure 2), matched as  $g_{\text{I}}J_z + g_{\text{S}}S_z$  value, is clearly consistent with  $J_z = \pm 15/2$  as  $\text{Dy}^{\text{III}}$  ground state,  $S_z = \pm 1/2$  as  $\text{Fe}^{\text{III}}_{\text{LS}}$  and  $g_{\text{I}} \sim 4/3$ ,  $g_{\text{S}} \sim 2$ .

The antiferromagnetic status shows that the  $d-f$  interaction is more than trough-space dipolar. The spin maps suggest a  $d-f$  exchange via the ligand  $\sigma$  skeleton rather than by  $\pi$  delocalization, explaining the low magnitude of the coupling. As an electron count rule, the doubly degenerate LF + SO driven levels determine the possibility of SMM effect. In the Ising scheme, the degenerate couples comprise opposite  $\pm J_z$  states, the exchange breaking the local Kramers symmetry. The reversal of magnetization occurs between degenerate Ising companions, encompassing a barrier related to the hard plane of the  $\text{Dy}^{\text{III}}$   $\chi$  tensor. We presented here the first ab initio account of ligand field, spin-orbit, and exchange effects in a  $d-f$  SMM system. The corroboration with the experiment implies compound **1** as a prototypic case study.

**Acknowledgment.** M.F. is indebted to JSPS (P04390) and T.K. to MECSSST Japan Grant-in-Aid. F.C. acknowledges the COE fellowship. M.F. and F.C. also thank to CNCSIS/RO (886 and 1422).

**Supporting Information Available:** Structural, magnetic, and computational details are available. This material is available free of charge via the Internet at <http://pubs.acs.org>.

## References

- (1) (a) Christou, G.; Gatteschi, D.; Hendrickson, D. N.; Sessoli, R. *MRS Bull.* **2000**, 25, 66–71. (b) Gatteschi, D.; Sessoli, R. *Angew. Chem., Int. Ed.* **2003**, 42, 268–297.
- (2) (a) Zaleski, C. M.; Depperman, E. C.; Kampf, J. W.; Kirk, M. L.; Pecoraro, V. L. *Angew. Chem., Int. Ed.* **2004**, 43, 3912–3914. (b) Mishra, A.; Wernsdorfer, W.; Abboud, K. A.; Christou, G. *J. Am. Chem. Soc.* **2004**, 126, 15648–15649.
- (3) Costes, J.-P.; Dahan F.; Wernsdorfer, W. *Inorg. Chem.* **2006**, 45, 5–7.
- (4) (a) Ishikawa, N.; Sugita, M.; Wernsdorfer, W. *J. Am. Chem. Soc.* **2005**, 127, 3650–3651. (b) Ishikawa, N.; Sugita, M.; Wernsdorfer, W. *Angew. Chem., Int. Ed.* **2005**, 44, 2931–2935.
- (5) Kajiwara, T.; Nakano, M.; Kaneko, Y.; Takaishi, S.; Ito, T.; Yamashita, M.; Igashira-Kamiyama, A.; Nojiri, H.; Ono, Y.; Kojima, N. *J. Am. Chem. Soc.* **2005**, 127, 10150–10151.
- (6) Crystal data for  $1 \cdot \text{H}_2\text{O} \cdot 4.5\text{MeNO}_2$ : triclinic,  $P\bar{1}$ ,  $a = 11.115(4)$  Å,  $b = 13.567(5)$  Å,  $c = 15.758(5)$  Å,  $\alpha = 103.462(7)^\circ$ ,  $\beta = 92.753(7)^\circ$ ,  $\gamma = 109.525(6)^\circ$ ,  $V = 2157.4(13)$  Å<sup>3</sup>,  $Z = 2$ ,  $T = 200(2)$  K,  $wR2 = 0.1315$  (6258 unique reflections),  $R1 = 0.057$  (5511 reflections with  $I > 2\sigma(I)$ ) using 651 parameters.
- (7) Calculations done with GAMESS: Schmidt, M. W.; Baldrige, K. K.; Boatz, J. A.; Elbert, S. T.; Gordon, M. S.; Jensen, J. H.; Koseki, S.; Matsunaga, N.; Nguyen, K. A.; Su, S. J.; Windus, T. L.; Dupuis, M.; Montgomery, J. A. *J. Comput. Chem.* **1993**, 14, 1347–1363.
- (8) Paulovic, J.; Cimpoesu, F.; Ferbinteanu, M.; Hirao, K. *J. Am. Chem. Soc.* **2004**, 126, 3321–3331.
- (9) Ishikawa, N.; Sugita, M.; Okubo, T.; Tanaka, N.; Iino, T.; Kaizu, Y. *Inorg. Chem.* **2003**, 42, 2440–2446. We took from this work  $[\text{Pc}_2\text{Ln}]^+$  complexes as calculation tests, obtaining excellent match of our CASSCF + SO results with the authors LF + SO fit to experiment.

JA062399I